

# BGM2Pose: Active 3D Human Pose Estimation with Non-Stationary Sounds

Yuto Shibata  
Keio University  
yuto071508@keio.jp

Yusuke Oumi  
Keio University  
youmi@keio.jp

Go Irie  
Tokyo University of Science  
goirie@ieee.org

Akisato Kimura  
NTT Corporation  
akisato@ieee.org

Yoshimitsu Aoki  
Keio University  
aoki@elec.keio.ac.jp

Mariko Isogawa  
Keio University, JST Presto  
mariko.isogawa@keio.jp

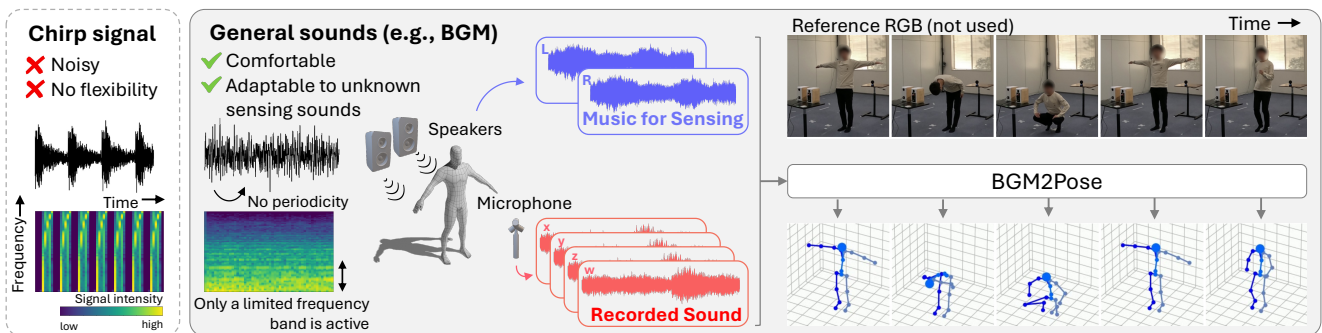


Figure 1. We propose BGM2Pose, a 3D human pose estimation that utilizes background music that naturally integrates into everyday life, for active acoustic sensing. Given playback music and recorded acoustic signals, our method estimates frame-by-frame 3D human poses. Unlike chirp signals, BGM tracks contain unstable sounds and limited frequency bands.

## Abstract

We propose BGM2Pose, a non-invasive 3D human pose estimation method using arbitrary music (e.g., background music) as active sensing signals. Unlike existing approaches that significantly limit practicality by employing intrusive chirp signals within the audible range, our method utilizes natural music that causes minimal discomfort to humans. Estimating human poses from standard music presents significant challenges. In contrast to sound sources specifically designed for measurement, regular music varies in both volume and pitch. These dynamic changes in signals caused by music are inevitably mixed with alterations in the sound field resulting from human motion, making it hard to extract reliable cues for pose estimation. To address these challenges, BGM2Pose introduces a Contrastive Pose Extraction Module that employs contrastive learning and hard negative sampling to eliminate musical components from the recorded data, isolating the pose information. Additionally, we propose a Frequency-wise Attention Module that enables the model to focus on subtle acoustic variations attributable to human movement by dynamically computing

attention across frequency bands. Experiments suggest that our method outperforms the existing methods, demonstrating substantial potential for real-world applications. Our datasets and code will be made publicly available.

## 1. Introduction

This paper tackles the challenging task of estimating human poses using common background music playing in a room, without relying on specialized sensing signals. Human pose estimation and activity recognition have been long-standing challenges in computer vision [5, 23, 31]. These technologies have diverse applications, including sports performance analysis [10, 44], rehabilitation [7, 29], and XR applications [37]. Although many effective methods have been proposed, most of them rely on RGB images or videos captured by standard cameras. These approaches face challenges such as vulnerability to occlusion and low-light conditions [21], as well as privacy concerns due to the capture of identifiable features like faces [12, 48].

Acoustic signals are one promising modality to address these challenges. They are less affected by lighting condi-

tions and, due to their longer wavelengths, are less likely to contain privacy-related information such as facial expressions. While other modalities with similar advantages (e.g., millimeter-wave or WiFi signals) also exist [11, 17, 32, 47], these signals often face restrictions in environments with medical equipment or on airplanes. By contrast, sound can be used almost anywhere.

Several methods using acoustic signals for human state estimation have been explored [34, 42]. Existing approaches utilize chirp signals where the frequency monotonically increases or decreases over time as the sensing source, which is also a common method in systems using wireless signals. Specifically, these approaches repeatedly emit the same chirp signal and observe changes in the signal to detect and estimate state changes caused by human movement. However, this method faces several limitations. First, chirp signals typically span a wide frequency range, including audible frequencies, making them highly uncomfortable for human ears. Second, a general constraint in methods using chirp signals—whether acoustic or otherwise—is the requirement to use the exact same sensing signal during inference as was used during training. Both conditions highly limit the method’s applicability in real-world scenarios.

Therefore, this paper addresses these challenges by proposing a task of **3D Human Pose Estimation Based on Non-Stationary Sounds** (Fig. 1), which significantly expands the framework of non-invasive estimation of dynamic human pose. In this task, we utilize standard background music (BGM) as the sensing signal. With BGM, our system significantly enhances comfort and practicality compared to a noisy, chirp-based framework. It also retains the advantages of acoustic sensing, including robustness to occlusion and dark environments, as well as privacy protection.

Utilizing everyday BGM as a sensing signal introduces several critical challenges: (i) human motion induces slight variations in the phase and amplitude of the collected audio data due to sound attenuation and reflection at the human body surface. In settings where the sensing signal itself varies significantly with music, these pose-related components can be overshadowed by changes in the music, creating a “*needle in a haystack*” challenge. To demonstrate how challenging this task is compared to methods using chirp signals, Fig. 2 visualizes the difference between recorded sounds when regular music and repeated chirp signals are used for human pose estimation. In this figure, the common acoustic features (*i.e.*, mel spectrogram and intensity vector) of recorded audio are mapped onto a two-dimensional space using principal component analysis (PCA), with different colors corresponding to different poses. The figure shows that with repeated chirp signals, signal changes are directly associated with changes in poses, forming pose patterns even without model training. In contrast, with the regular music we use, it becomes significantly difficult to ex-

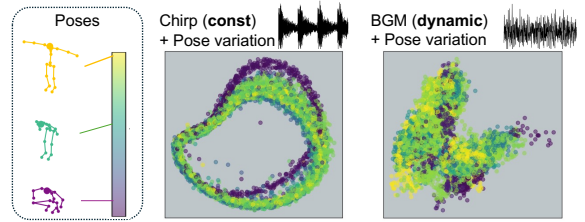


Figure 2. **Acoustic feature visualization.** (Left) With the repeated chirp signals, differences in collected audio data correspond directly to pose changes, forming patterns for each pose. (Right) In our setting, changes in BGM overshadow human pose variation.

tract pose information since the changes in poses are largely obscured by the fluctuations in the music. We strongly recommend watching the supplementary material videos with audio to understand the system overview and to grasp the magnitude of variation in the sensing signals. (ii) unlike chirp signals that sweep across a wide range of frequencies, BGM has a limited frequency band that changes over time (see Fig. 1). Since pose information is observed as changes occurring within the BGM, the model needs to selectively attend to the relevant portions of the spectrogram. (iii) since this framework does not assume specific predefined signals such as chirp, the method needs to adapt to unseen acoustic signals for inference.

To address these challenges, we propose a novel model called BGM2Pose. To overcome the first challenge of separating sound variations caused by the non-periodic source and the human pose, we introduce a Contrastive Pose Extraction module (CPE module). This module effectively promotes the extraction of pose components while simultaneously excluding music components by employing a contrastive loss within a shared feature space. To address the second challenge of limited frequency bands and the third challenge of generalizing to unseen acoustic signals, we incorporate a Frequency-wise Attention Module (FA module). This module uses an attention mechanism to effectively identify the frequency bands of the spectrogram containing human pose information from the recorded signal, allowing it to extract posture-estimation-relevant information even from limited frequency bands or unseen music.

Since no existing work has addressed inferring 3D human poses with BGM, we create Acoustic Music-based Pose Learning (AMPL) dataset, a large-scale original dataset for this task. Following [34], we set up an active acoustic-sensing system using a single pair of ambisonics microphones and loudspeakers. We then actively record the acoustic signals in which BGM and human movement-caused signals are mixed. These signals are synchronized with motion capture (Mocap) data and captured in an ordinal classroom environment with a certain level of noise.

Our contributions are summarized as follows: (1) for the first time, we propose the task of 3D human pose estimation using BGM that blends into daily life; (2) we introduce a framework that directly maps acoustic signals, in which

Table 1. Comparisons between existing human-pose-related studies and our method.

Task	Method	Modality	Comfort	Restricted Usage	Inference Signal
Pose Estimation	RGB-based [5, 23, 31]	RGB	Low (privacy concerns)	Dark environment, occlusion	-
	RF/WiFi-based [17, 22, 32, 47]	RF/WiFi	High	Occlusion, electronic device	Fixed
	Audio2Hand [20, 27, 46]	Audio	Low (invasive)	Soundproof environment	Fixed
	Sound2Pose [34, 42]	Audio	Low (chirp signals)	Soundproof environment	Fixed
	BGM2Pose(Ours)	Audio	High	Soundproof environment	Adaptive
Motion Generation	Music2Motion [35, 38]	Audio	High	Inapplicable for sensing	-
	Speech2Pose [13, 41, 45, 49]	Audio	High	Inapplicable for sensing	-

BGM- and human-movement-caused signals are mixed, to 3D human poses; (3) we introduce our CPE module, which employs a contrastive loss to encourage the model to extract only pose information from the collected audio, and our FA module, which dynamically calculates attention to focus on specific frequency bands conditioned on sensing sounds; and (4) we construct the AMPL dataset, a novel dataset using four BGM tracks spanning two different genres as sensing signals.

## 2. Related Work

Table 1 summarizes where our method is positioned among the existing studies relevant to ours. This section describes them and highlights their differences with our approach.

**Human Pose Estimation with Different Modalities.** Human pose estimation is a traditional task in computer vision and has gained much attention due to its broad applications. Many studies have featured RGB-based models, since human pose can be perceived easily through cameras. However, using RGB images or videos can lead to reduced accuracy in cases of occlusion or poor lighting, and the large amount of visual information they contain also raises concerns over privacy [12, 48]. With the help of advanced deep learning techniques, the use of other modalities, such as WiFi/RF and mmWave, has also been rapidly increasing [11, 17, 22, 32, 47]. While these modalities can perform well in dark environments, there are some limitations regarding their use in settings with precise instruments, such as in hospitals or during flights. Furthermore, certain materials such as water or metal lead to occlusion issues for these modalities. We will address these limitations by utilizing acoustic signals for 3D human pose estimation.

**Active Acoustic Sensing.** Acoustic signals, which have significantly lower frequencies than the signals mentioned above, are subject to fewer usage restrictions. Additionally, acoustic signals, due to their long wavelengths, can transmit information even in environments with obstacles. Inspired by bats’ spatial recognition abilities, [6] achieved room-depth estimation based on acoustic signals and two microphones. Indoor human position estimation was also conducted using sine sweeps and music [39]. Although not focused on sensing, previous studies [16, 40] analyzed the relationship between 3D human poses and the nearby sound

field as part of an acoustic scene rendering task. Regarding the human pose estimation, some prior studies have successfully predicted joint positions using either RGB images and acoustic signals [42] or solely multi-channel acoustic signals [28, 34]. However, all previous works have utilized mathematically optimized chirp signals to investigate echo characteristics, and these systems are impractical considering that chirp signals contain distracting, audible noise within the human hearing range (see Fig. 1 (left)). Other studies tackling active hand/upper-body pose estimation based on acoustic signals required users to put on wearable devices [20, 25, 27, 46], which is not practical in real-life scenarios. For more practical human sensing, we utilize nonengineered BGM for noninvasive active sensing.

**Avatar Synthesis from Music Sound.** A line of research on human pose generation includes the Sound to Avatar task [13, 35]. With the advances in generative models such as diffusion models [15, 36], the number of studies of avatar creation based on sound semantics, such as speech or music, is increasing [38, 49]. However, please note that these tasks involving generating “semantically plausible” poses by leveraging the semantics of sounds are entirely different from our task, which estimates “physically correct” poses using sound as measurement signals.

## 3. Methodology

Our goal is to estimate the 3D human pose sequence  $\{\mathbf{p}_t\}_{t=1}^T$  of a target subject standing between a microphone and loudspeakers, given the recorded sound sequence  $\{\mathbf{s}_t\}_{t=1}^T$  and original music sequences  $\{\mathbf{m}_{i,t}\}_{t=1}^T$  emitted from the  $i$ -th speakers. Here,  $T$  indicates the length of input and output sequences and  $t$  means each timestep. We assume a typical consumer speaker setup with two speakers (*i.e.*, right and left). Following [34], we also use one ambisonics microphone, which captures omnidirectional (w) and x, y, and z components with four channels in B-Format.

An overview of our BGM2Pose method is shown in Fig. 3. Our framework includes three main components: an acoustic feature extraction module, the Frequency-wise Attention (FA) module, and the Contrastive Pose Extraction (CPE) module. The FA module enables the model to focus on subtle acoustic variations caused by human posture by dynamically applying attention across frequency bands.

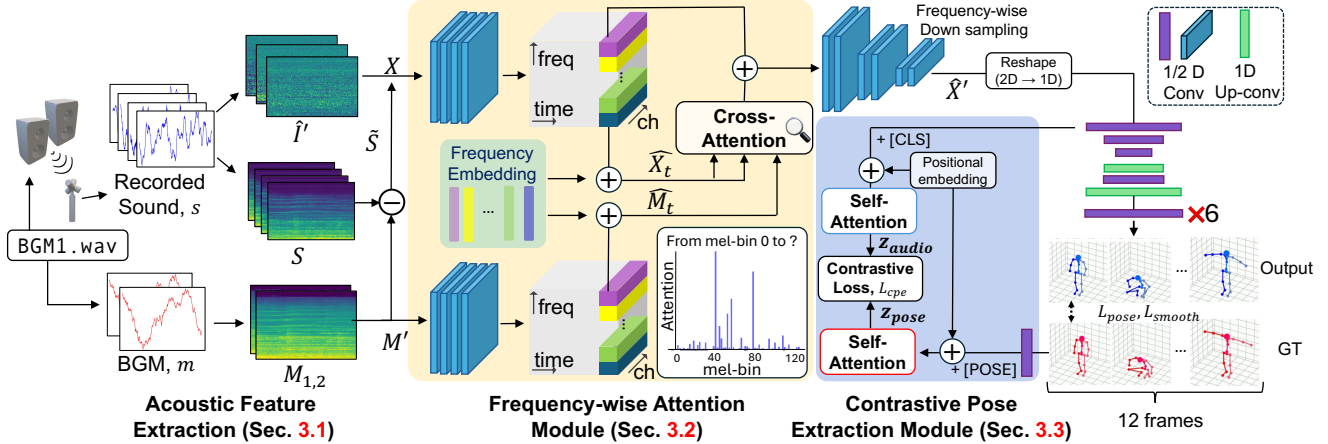


Figure 3. The overview of our framework for BGM-based 3D human pose estimation.

The CPE module then uses contrastive learning on the embeddings of recorded audio and pose, which encourages the model to extract pose components from the audio data while eliminating sensing music effects.

Acoustic feature engineering is described in Sec. 3.1. Secs. 3.2 and 3.3 explain our main technical contributions—namely, the FA module and the CPE module, respectively. Then, Sec. 3.4 describes our loss functions.

### 3.1. Acoustic Feature Extraction

To generate the sequence of the audio feature vectors as the input to our framework, one straightforward way is to directly feed raw signals into some networks for audio feature learning. However, following [13, 34], which showed the efficacy of feature engineering before feeding signals into a network, we generate three types of acoustic features. From the recorded sound signals  $s_t$ , we extract the intensity vector  $\mathbf{I}_{\text{intensity}} \in \mathbb{R}^{3 \times b \times T}$ , including three channels of  $(x, y, z)$ -directional components, and the log-mel spectrum  $\mathbf{S}_{\text{logmel}} \in \mathbb{R}^{4 \times b \times T}$ . Here,  $b$  denotes the number of frequency bins. These features are often used for sound source localization [43] and audio event detection [19], respectively. Given the original BGM sound signals  $\mathbf{m}_i$  emitted from the left and right speakers, we generate the log-mel spectrum  $\mathbf{M}_{\text{logmel}} \in \mathbb{R}^{2 \times b \times T}$ . Since the range of each signal is different between the intensity vector and log Mel spectrogram, we standardized them before concatenation. In our implementation, we use  $b = 128$  and  $T = 12$ .

**The intensity vector** is the feature that is often used for the direction of arrival (DOA) estimation [30, 43] since it represents the acoustical energy direction of signals. We utilize this feature to obtain clues for perceiving the scene geometry including human 3D poses. Intensity vector is computed as follows:

$$\hat{\mathbf{I}}_{f,t} = \mathcal{R} \left\{ \mathbf{W}_{f,t}^* \cdot \begin{pmatrix} \mathbf{X}_{f,t} \\ \mathbf{Y}_{f,t} \\ \mathbf{Z}_{f,t} \end{pmatrix} \right\}, \quad (1)$$

$$\hat{\mathbf{I}}'_{k,t} = \mathbf{H}_{k,f} \frac{\hat{\mathbf{I}}_{f,t}}{\|\hat{\mathbf{I}}_{f,t}\|_2}, \quad (2)$$

where  $\mathbf{W}, \mathbf{X}, \mathbf{Y}, \mathbf{Z}$  are the STFT (Short Time Fourier Transform) domain of  $w, x, y, z$ , respectively.  $\mathbf{H}$  represents the Mel-bank filter, and  $k$  is the index of the Mel bins.  $\mathcal{R}\{\cdot\}$  indicates the real part,  $*$  denotes the conjugate, and  $\|\cdot\|$  represents the  $L1$  norm.

**The log-mel Spectrum** is an acoustic time-frequency representation and is known for its good performance as the input of a convolutional neural network [26, 33]. STFT is performed for the received audio signal  $s_t$  or the original music sound signal  $\mathbf{m}_t$ , and we apply mel filter bank and logarithmic transformation to compute  $\mathbf{S}_{k,t}, \mathbf{M}_{k,t}$ .

To filter out the influence of BGM from our recorded audio, we explicitly subtract the original music data  $\mathbf{M}_i$ , emitted from the  $i$ -th speaker, from the recorded audio data  $\mathbf{S}$  after standard normalization. Then, sound difference features  $\hat{\mathbf{S}}$  are calculated as follows:

$$\hat{\mathbf{S}}_{i,c,k,t} = \mathbf{S}'_{c,k,t} - \mathbf{M}'_{i,k,t}. \quad (3)$$

Here,  $c$  denotes the channel, and  $\mathbf{S}'$  and  $\mathbf{M}'_i$  represent the log-mel spectrograms after channel-wise normalization for recorded sounds and music sounds emitted from  $i$ -th speaker, respectively. Subtraction in a log scale is equal to division in a linear scale, which means this module calculates the pseudo transfer functions. By concatenating the intensity vector and these difference features with two speakers, we obtain the feature  $\mathbf{X}$  with  $4 + 4 + 3 = 11$  channels in total, which is fed into our network model.

### 3.2. Frequency-wise Attention Module

To effectively extract acoustic changes caused by human posture in response to dynamic sensing signals, our method proposes a Frequency-wise Attention Module (FA module). Unlike TSP (chirp) signals designed to emit signals with

constant intensity across all frequencies within a specific time frame, the frequency in BGM does not have periodicity and varies over time (see Fig. 1 (left)). Given that human pose information is observed as changes occurring within the sensing sound, accurately estimating poses requires identifying the frequency bands in the spectrogram that contain the sensing music and are effective for pose estimation. At the same time, the frequency-wise downsampling via convolutional operation at the earlier stages may risk blending information from frequency bands unrelated to the playing sound, potentially leading to reduced accuracy. Therefore, we compute the frequency-wise attention for the input features in accordance with the sensing BGM features while maintaining the original frequency resolution at the earlier stages of the model.

The FA module takes acoustic feature  $\mathbf{X}$  and the music feature  $\mathbf{M}$  as input. To aggregate local information of the inputs, we independently apply 2D CNNs to both  $\mathbf{X}$  and  $\mathbf{M}$ . Here, we do not apply any downsampling to keep the original frequency resolution. Then, we obtain the recorded sound feature  $\mathbf{X}'_t \in \mathbb{R}^{b \times d}$  and the music feature  $\mathbf{M}'_t \in \mathbb{R}^{b \times d}$  for each time index  $t$ , where  $d$  is the latent dimension.

Because the attenuation and diffraction characteristics of sound vary depending on frequency, we add learnable shared frequency embedding  $\mathbf{F} \in \mathbb{R}^{b \times d}$  to the aforementioned two features,  $\hat{\mathbf{X}}_t = \mathbf{X}'_t + \mathbf{F}$  and  $\hat{\mathbf{M}}_t = \mathbf{M}'_t + \mathbf{F}$ . Then, the attention mechanism is calculated as follows:

$$\text{Attention}(\mathbf{Q}_t, \mathbf{K}_t, \mathbf{V}_t) = \text{softmax}\left(\frac{\mathbf{Q}_t \cdot \mathbf{K}_t^T}{\sqrt{d}}\right)\mathbf{V}_t, \quad (4)$$

where  $\mathbf{K}_t = \hat{\mathbf{M}}_t \mathbf{W}^K$ ,  $\mathbf{Q}_t = \hat{\mathbf{X}}_t \mathbf{W}^Q$ , and  $\mathbf{V}_t = \hat{\mathbf{X}}_t \mathbf{W}^V$ . Here,  $\mathbf{W}^K$ ,  $\mathbf{W}^Q$ , and  $\mathbf{W}^V \in \mathbb{R}^{d \times d}$  are the key, query, and value projection matrices, respectively. Since both human movement and music changes are continuous and have little long-term dependency, we do not calculate temporal attention. To preserve the time consistency brought by upstream 2D CNN layers, we leverage a residual connection [14] followed by 2D CNNs, which involve the frequency-wise downsampling to get feature  $\hat{\mathbf{X}}'$ . Then,  $\hat{\mathbf{X}}'$  is fed into a reshaping layer, a time-wise 1D U-Net module, and 1D CNN layers to output pose  $\mathbf{p}$  with a size of  $12 \times 63$ , which consists of  $3D \times 21$  joints for each of the 12 frames. For the number of convolutional layers, please refer to Fig. 3.

### 3.3. Contrastive Pose Extraction Module

To mitigate the influence of sensing music on the model’s representations and to enable the extraction of pose information only, we propose a Contrastive Pose Extraction module (CPE module) based on contrastive learning (Fig. 4). This module is designed to incur a high loss when the model’s output is influenced by the sensing BGM. This module performs multi-modal contrastive learning that

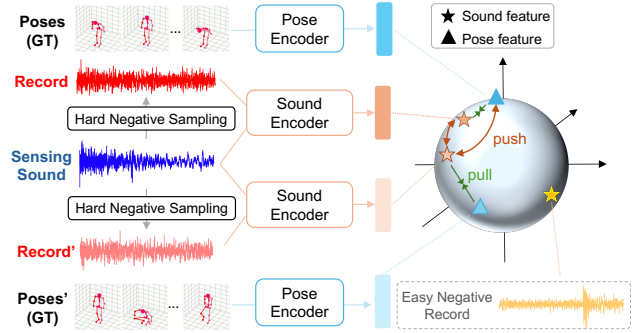


Figure 4. We perform contrastive learning using encoded pose sequences and recorded audio features to achieve feature extraction that is independent of the BGM.

maps human poses and recorded audio into a common feature space. In this contrastive learning framework, the model is trained in each minibatch to bring positive pairs (i.e., each pose sequence and its corresponding recorded audio) closer in the feature space while pushing negative pairs farther apart. When samples recorded with similar sensing music are included in the same mini-batch, the learning process encourages separating them, thereby promoting the extraction of only pose information. Additionally, we propose a novel sampling method called “BGM-based hard negative sampling.” In this approach, similar recordings (and corresponding pose data) obtained using the same sensing BGM are included in the same mini-batch, imposing a more challenging setting for contrastive learning to further enhance the model’s discriminative ability (see two similar red and one dissimilar yellow recordings in 4).

For multi-modal contrastive learning, it is necessary to prepare embeddings for both pose sequences and acoustic features. Following the approach of BERT [8] and Vision Transformer [9], we represent each embedding with a learnable token, [POSE] and [CLS], respectively. For the pose sequence  $\{\mathbf{p}_t\}_{t=1}^T$ , after adjusting the dimensions through a 1D convolution layer, it is concatenated with the [POSE] token and combined with a learnable time embedding. For acoustic features, as shown in Fig. 3, they are reshaped to 1D and passed through a convolutional layer, then concatenated with the [CLS] token and combined with the time embedding. For each modality, we apply a single layer of self-attention to aggregate temporal information, after which we extract the [POSE] and [CLS] tokens. These outputs are normalized to map onto a hypersphere and expressed as  $\mathbf{z}_{\text{pose}}$  and  $\mathbf{z}_{\text{audio}}$ , respectively.

With  $\langle \cdot, \cdot \rangle$  denoting the inner product and the temperature  $\tau$ , the cosine similarity  $s_{i,j}$  between  $i$ -th pose and  $j$ -th audio sequences and our contrastive loss are expressed as follows:

$$s_{i,j} = \langle \mathbf{z}_{\text{pose}_i}, \mathbf{z}_{\text{audio}_j} \rangle \quad (5)$$

Table 2. Details of the proposed AMPL dataset.

Name	Genre	Duration	Subject IDs
ARNOR [1]	Ambient	11:12	[1, 1, 2, 3, 4, 5, 9]
Cirrus [2]	Ambient	6:58	[1, 1, 2, 3, 4, 5, 6, 7, 8, 9]
MANTRA [4]	Ambient	8:37	[1, 1, 2, 3, 4, 5, 9]
Kurina blues [3]	Jazz	14:44	[6, 7, 8]

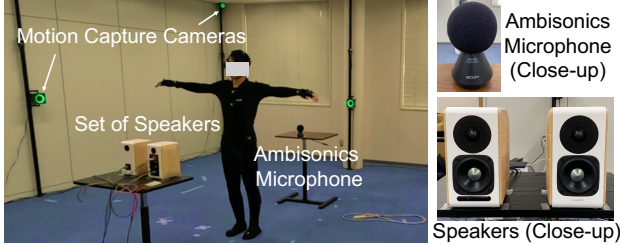


Figure 5. The setup of our experiments.

$$L_{cpe} = \frac{1}{2N} \sum_{i=1}^N \left[ -\log \frac{\exp(s_{i,i}/\tau)}{\sum_{k=1}^N \exp(s_{i,k}/\tau)} - \log \frac{\exp(s_{i,i}/\tau)}{\sum_{k=1}^N \exp(s_{k,i}/\tau)} \right] \quad (6)$$

### 3.4. Other Loss Function

Similar to previous methods [17, 34], our network is also trained using loss functions designed to address the correctness and smoothness of the poses. The pose loss measures the Mean Squared Error (MSE) between the  $j$ -th predicted and ground truth joint position of  $i$ -th subject at timestamp  $t$  (i.e.,  $p_{i,t,j}$  and  $\hat{p}_{i,t,j}$ , respectively).

$$\mathcal{L}_{pose}(\theta) = \frac{1}{TNJ} \sum_{i=0}^N \sum_{t=0}^T \sum_{j=0}^J (\hat{p}_{i,t,j} - p_{i,t,j})^2 \quad (7)$$

Here,  $\mathcal{L}$  denotes the loss function,  $\theta$  represents trainable parameters and  $J$  is the total joint size. We also use the smooth loss to make our prediction smoother.

$$\mathcal{L}_{smooth}(\theta) = \frac{1}{(T-1)} \sum_{t=2}^T \text{MSE}((\hat{\mathbf{p}}_t - \hat{\mathbf{p}}_{t-1}) - (\mathbf{p}_t - \mathbf{p}_{t-1})). \quad (8)$$

With weight parameters  $w_\alpha$  and  $w_\beta$ , our total loss function is as follows:

$$L = L_{pose} + w_\alpha L_{smooth} + w_\beta L_{cpe} \quad (9)$$

## 4. Human Pose Dataset with Music

For our task, we created a large-scale dataset, **AMPL** (**A**coustic **M**usic-based **P**ose **L**earning dataset), which links musical sensing signals with 3D human poses. These data are captured in a classroom environment, which includes background noise and reverberation, using motion capture (Mocap) and 16 cameras. For the right and left speakers, we used Edifier ED-S880DB, commercial high-resolution speakers. Additionally, we captured acoustic signals using an ambisonics microphone (Zoom H3-VR). As shown in

Fig. 5, the speakers and microphone were placed one meter away from the subjects, who were positioned in the line of sight. For details on the recording environment, please refer to the supplementary materials.

Table 2 summarizes detailed information on the BGM used for sensing, including titles, genres, duration, and target subjects. The ambient music tracks have short silent intervals, although there are intra/inter differences in the music tracks in their pitch and volume. The subjects performed various poses, such as standing still, bending, and walking. We shifted and normalized each joint position so that the hips were positioned at the origin of our coordinates, and the spine-hip distance was set as 1. To investigate the effect of the sound absorption properties of clothing, two subjects wore their personal outfits (the subject IDs indicated in red). Since these data were collected without putting Mocap markers on their clothes, these data lack ground-truth pose information. Therefore, these data were used only for qualitative evaluation.

## 5. Experimental Settings

**Baselines** So far, no existing method has performed 3D human pose estimation using both music and recorded data as inputs. Therefore, we compared our model against the following approaches that are similar to ours; (i) **Jiang et al.** [17] that uses WiFi signals, but like us, they use actively acquired low-dimensional data as input. (ii) **Ginosar et al.** [13], which uses acoustic modality, similar to our approach, but focuses on gesture generation with audio that contains semantics, such as human speech. (iii) **Shibata et al.** [34], which is most relevant to ours in the sense that they use acoustic signals for 3D human pose estimation, but they assume chirp sound as active sensing signals. **Please note that all baseline models were trained on our dataset for fair architecture comparisons.** To this end, we modified the input and final layers of each baseline network to accept our acoustic signals as input and output 3D human poses.

**Evaluation Metrics** Our quantitative metrics are as follows: root mean square error (RMSE), mean absolute error (MAE), and percentage of correct key point (PCK). RMSE and MAE are used to express the average displacement between the predicted and the true joint positions, while PCK indicates the percentage of the model’s predictions that fall within a predefined threshold from the correct positions. In particular, we use the PCKh@0.5 score with a threshold of 50% for the head–neck bone link.

**Implementation Details** To synchronize the playback music with the collected sound data, the playback music were upsampled from 44,100 Hz to 48,000 Hz. Regarding the acoustic features, sampling was conducted to achieve a frame rate of 20 FPS. For training, we used Adam [18] for optimization and employed a cosine annealing learning

Table 3. Quantitative experimental results in the (a) single-music and the (b) cross-music settings.

Method	(a) Single-Music			(b) Cross-Music		
	RMSE	MAE	PCKh @0.5	RMSE	MAE	PCKh @0.5
	(↓)	(↓)	(↑)	(↓)	(↓)	(↑)
Jiang <i>et al.</i> [17]	1.338	0.768	0.251	1.417	0.800	0.272
Ginosar <i>et al.</i> [13]	1.223	0.666	0.379	1.274	0.682	0.375
Shibata <i>et al.</i> [34]	1.090	0.574	0.468	1.110	0.556	0.499
Ours	<b>0.923</b>	<b>0.453</b>	<b>0.573</b>	<b>1.036</b>	<b>0.494</b>	<b>0.570</b>

Table 4. Quantitative experimental results with (c) cross-genre setting (train=ambient, test=jazz).

Method	RMSE (↓)	MAE (↓)	PCKh@0.5 (↑)
Jiang <i>et al.</i> [17]	1.418	0.849	0.221
Ginosar <i>et al.</i> [13]	1.326	0.727	0.360
Shibata <i>et al.</i> [34]	1.112	0.595	0.376
Ours	<b>1.065</b>	<b>0.543</b>	<b>0.463</b>

scheduler [24], which reduced the learning rate from 0.003 to 0.001. All training was conducted using exponentially moving average for model updates. The batch size was set to 64. All models were trained for 30 epochs. Regarding the weights in Eq. 9, we set  $w_\alpha = 100$  and  $w_\beta = 1$ . In this main paper, the temperature  $\tau$  is set to 0.07.

## 6. Experimental Results

We conducted four experiments to investigate the effectiveness of the proposed method: (1) a comparison with the aforementioned baselines; (2) an ablation study to show the efficacy of the CPE module and the FA module, which are our main technical contributions. To verify effectiveness under real-world conditions, (3) we investigated the proposed method’s robustness against noise present in recorded sound data. While these experiments used a motion capture suit dataset that included ground truth, (4) we conducted qualitative analysis with the “in Plain Clothes” dataset to further showcase our method’s applicability. For additional experiments, including temperature  $\tau$  sensitivity and multi-channel effects, please refer to the supplementary material.

### 6.1. Comparison with Other Baselines

We evaluated our proposed method against the aforementioned models within the following three distinct scenarios: (a) a single-music setting, wherein the same ambient BGM was used as the acoustic source for both training and testing; (b) a cross-music setting, in which two ambient and one jazz BGM were used for training and the remaining ambient music was used for testing only; and (c) a cross-genre setting, in which all ambient tracks were used for training and one jazz BGM was used for testing. Regarding (a) and (b), only ambient tracks were used for testing since they have few silence intervals and are suitable for stable evaluation

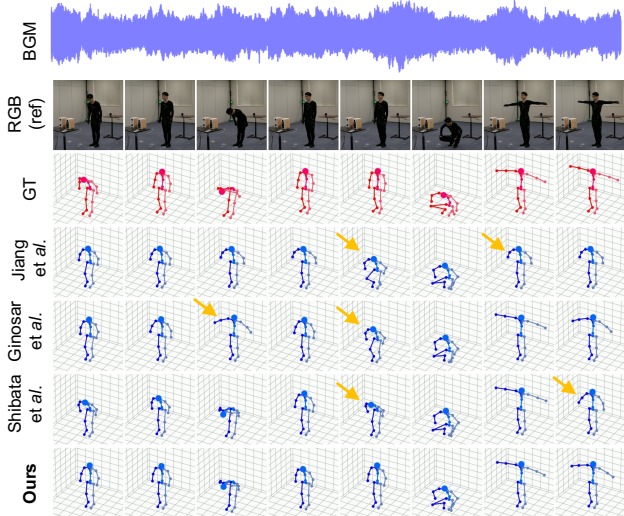


Figure 6. The qualitative results with the Mocap suit under the single-music setting.

Table 5. Ablation study in the single- and the cross-music settings.

Method	(a) Single Music			(b) Cross Music		
	RMSE	MAE	PCKh @0.5	RMSE	MAE	PCKh @0.5
	(↓)	(↓)	(↑)	(↓)	(↓)	(↑)
Ours	<b>0.923</b>	<b>0.453</b>	<b>0.573</b>	1.036	<b>0.494</b>	<b>0.570</b>
w/o CPE module	0.945	0.481	0.531	<b>1.024</b>	0.501	0.547
w/o BGM Hard Negative	0.928	0.457	0.566	1.065	0.506	0.559
w/o FA module	1.025	0.509	0.536	1.210	0.593	0.512
w/o BGM conditioning	0.970	0.484	0.537	1.075	0.522	0.543

compared to jazz BGM. (b) and (c) are settings designed to evaluate the model’s generalization performance to unseen music and to both unseen music and genres, respectively.

The relationship between the music used for data collection and the subjects is shown in Table 2. For experimental settings (a) and (b), we conducted accuracy evaluations using K-fold cross-validation (K=5) on subjects with IDs 1–5, who completed data collection with all prepared ambient audio sources. The remaining three subjects, who collected data with “Cirrus” and “Jazz”, were also included in the training data for the Single-Music setting with “Cirrus” and for the Cross-Music setting with all three ambient tracks. In the Cross-Genre setting, we conducted three-fold cross-validation, using subjects [6, 7, 8] for evaluation and the remaining subjects’ data for training. Please note that across all BGM settings, we evaluated the model’s accuracy on subjects who were unseen during the training phase. For evaluation settings (a) and (b), the reported accuracy is the average across the three ambient music tracks. Additionally, to facilitate more effective accuracy comparisons, all experiments report accuracies averaged over three random seeds. For tables that include standard deviations, please refer to the supplementary material.

Table 3 summarizes the quantitative results in both the

single- and cross-music settings. We can see that our proposed method outperformed the previous models in all metrics under both settings, highlighting that it has a strong capacity to capture 3D human poses based on music sounds. Please note that the values in the table are normalized, with the hip-spine distance set to 1. In our Mocap system, with the spine position closest to the hip, the average of this distance across the 8 subjects was 9.21 cm. In particular, regarding PCKh@0.5, the proposed method outperforms the second-best approach by approximately 10% and 7% in both settings, suggesting that our method accurately identifies challenging poses, such as the ‘‘T-pose’’.

Table 4 shows the results when three ambient music tracks are used for training while jazz music is used for testing. Jazz exhibits more drastic changes in pitch and volume compared to ambient music, and it includes silent intervals during which the sensing signal does not work. Consequently, we observe a decrease in accuracy in PCKh@0.5 compared to evaluations conducted with ambient music (Table 3). However, even so, our method records significantly higher accuracy than existing methods, suggesting that our approach is robust across different music genres.

Fig. 6 shows the qualitative results for every 10 seconds under the single-music setting. The baseline methods failed to predict various poses, as shown by the yellow arrows, partly due to the effects of dynamic BGM. On the other hand, our method successfully predicted stable pose sequences, including T-pose, which had a very small area of acoustic reflection. For the qualitative results in the cross-music setting, please refer to the supplemental material.

## 6.2. Ablative Analysis

We investigated the effects of our main technical contributions, *i.e.*, the CPE module and the FA module. For the CPE module, we also prepared a setting in which mini-batches are created randomly without using proposed hard negative sampling. Furthermore, to demonstrate the effectiveness of using playback music in our method, we conducted accuracy evaluations in a setting where we removed the playback BGM channels (right/left) from the inputs and calculated FA module based on self-attention. Table 5 shows that both our proposed modules contributed to improving the estimation accuracy.

## 6.3. Noise Robustness Investigation

It is important to investigate the noise robustness of the method when considering applications in real-world environments. Table 6 shows the results in a single-music setting with Gaussian noise added to the collected sound data of both the training and test datasets. Here, SNR (Signal-to-noise ratio) is 10. Our method showed robustness to noise, achieving significantly higher estimation accuracy than existing methods by a large margin.

Table 6. Noisy environment setting (SNR=10).

Model	RMSE(↓)	MAE(↓)	PCKh@0.5(↓)
Jiang <i>et al.</i> [17]	1.567	0.931	0.095
Ginosar <i>et al.</i> [13]	1.389	0.796	0.262
Shibata <i>et al.</i> [34]	1.328	0.737	0.354
Ours	<b>1.202</b>	<b>0.637</b>	<b>0.430</b>

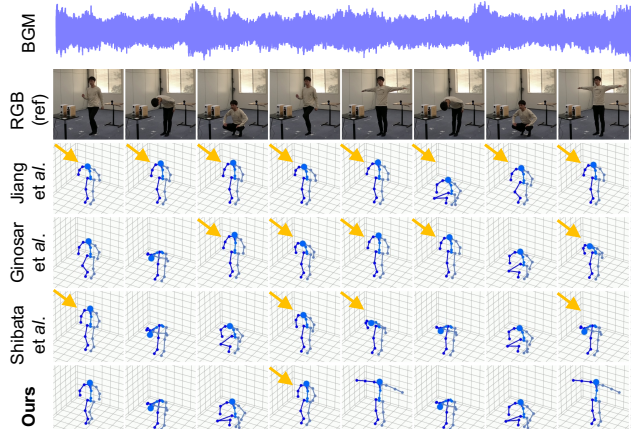


Figure 7. The qualitative results in the cross-music setting with the subjects wearing plain clothes.

## 6.4. Evaluation with the In Plain Clothes Dataset

Fig. 7 shows the qualitative results for every 16 seconds under the cross-music setting with the subject wearing plain clothes. As highlighted by the yellow arrows, we can see that our proposed method significantly reduced false predictions, compared to the baselines. The results indicate that the proposed method was robust to variations in the clothing worn by the subjects, although all the training data were captured with subjects putting on Mocap suits.

## 6.5. Discussion and Limitations

One of the main limitations of our framework is the requirement for the subject to stand in the line of sight of the microphone and the speaker, as shown in Fig. 5. This constraint arises from our goal of establishing a baseline under conditions in which the reflective surface area on a subject’s body is maximized, as a first step. Another limitation is its difficulty in accurately distinguishing between the left and right sides during walking actions.

## 7. Conclusion

This paper proposes BGM2Pose, a human 3D pose estimation that uses BGM as active sensing signals. Unlike existing methods that utilize specific chirp signals which is uncomfortable for humans, our approach uses everyday music, offering greater flexibility and practicality. This task is inherently challenging because the amplitude and pitch of the signals vary over time, and the human pose clues in recorded sounds are concealed by music changes. Moreover, the effective frequency range of BGM is lim-



ited. Therefore, we proposed a novel model incorporating the Frequency-wise Attention Module and the Contrastive Pose Extraction Module to focus on the changes in the measurement sounds caused by human pose variations at each moment. The proposed method demonstrated the ability to accurately estimate human 3D poses across a wide range of conditions, including unseen test music not used in the training data and unseen subjects wearing plain clothes. We hope that our research will lead to the development of human sensing applications using practical sounds.

**Acknowledgements.** This work was partially supported by JST Presto JPMJPR22C1, JSPS KAKENHI Grant Number 24K22296, and Keio University Academic Development Funds.

## References

- [1] Download link for the sensing music “armor”. <https://www.chosic.com/download-audio/32068/>. 6
- [2] Download link for the sensing music “cirrus”. <https://www.chosic.com/download-audio/54447/>. 6
- [3] Download link for the sensing music “kurina blues”. [https://freemusicarchive.org/music/Jazz\\_at\\_Mladost\\_Club/Jazz\\_Night/Kurina\\_blues/](https://freemusicarchive.org/music/Jazz_at_Mladost_Club/Jazz_Night/Kurina_blues/). 6
- [4] Download link for the sensing music “mantra”. <https://www.chosic.com/download-audio/42116/>. 6
- [5] Zhe Cao, Gines Hidalgo, Tomas Simon, Shih-En Wei, and Yaser Sheikh. OpenPose: Realtime multi-person 2D pose estimation using part affinity fields. *IEEE Transactions on Pattern Analysis and Machine Intelligence (TPAMI)*, 43(1): 172–186, 2021. 1, 3
- [6] Jesper Haahr Christensen, Sascha Hornauer, and X Yu Stella. Batvision: Learning to see 3d spatial layout with two ears. In *IEEE International Conference on Robotics and Automation (ICRA)*, pages 1581–1587, 2020. 3
- [7] R James Cotton, Allison DeLillo, Anthony Cimorelli, Kunal Shah, JD Peiffer, Shawana Anarwala, Kayan Abdou, and Tasos Karakostas. Markerless motion capture and biomechanical analysis pipeline. *arXiv preprint arXiv:2303.10654*, 2023. 1
- [8] Jacob Devlin. Bert: Pre-training of deep bidirectional transformers for language understanding. *arXiv preprint arXiv:1810.04805*, 2018. 5
- [9] Alexey Dosovitskiy, Lucas Beyer, Alexander Kolesnikov, Dirk Weissenborn, Xiaohua Zhai, Thomas Unterthiner, Mostafa Dehghani, Matthias Minderer, Georg Heigold, Sylvain Gelly, Jakob Uszkoreit, and Neil Houlsby. An image is worth 16x16 words: Transformers for image recognition at scale. *arXiv preprint arXiv:2010.11929*, 2021. 5
- [10] Sai Kumar Dwivedi, Yu Sun, Priyanka Patel, Yao Feng, and Michael J Black. Tokenhmr: Advancing human mesh recovery with a tokenized pose representation. In *IEEE/CVF Computer Vision and Pattern Recognition Conference (CVPR)*, pages 1323–1333, 2024. 1
- [11] Junqiao Fan, Jianfei Yang, Yuecong Xu, and Lihua Xie. Diffusion model is a good pose estimator from 3d rf-vision. In *European Conference on Computer Vision (ECCV)*, pages 1–18. Springer, 2025. 2, 3
- [12] Matt Fredrikson, Somesh Jha, and Thomas Ristenpart. Model inversion attacks that exploit confidence information and basic countermeasures. In *ACM Conference on Computer and Communications Security (CCS)*, pages 1322–1333, 2015. 1, 3
- [13] Shiry Ginosar, Amir Bar, Gefen Kohavi, Caroline Chan, Andrew Owens, and Jitendra Malik. Learning individual styles of conversational gesture. In *IEEE/CVF Computer Vision and Pattern Recognition Conference (CVPR)*, pages 3497–3506, 2019. 3, 4, 6, 7, 8
- [14] Kaiming He, Xiangyu Zhang, Shaoqing Ren, and Jian Sun. Deep residual learning for image recognition. In *IEEE/CVF Computer Vision and Pattern Recognition Conference (CVPR)*, pages 770–778, 2016. 5
- [15] Jonathan Ho, Ajay Jain, and Pieter Abbeel. Denoising diffusion probabilistic models. In *Conference on Neural Information Processing Systems (NeurIPS)*, pages 6840–6851, 2020. 3
- [16] Chao Huang, Dejan Markovic, Chenliang Xu, and Alexander Richard. Modeling and driving human body soundfields through acoustic primitives. In *European Conference on Computer Vision (ECCV)*, pages 1–17, 2024. 3
- [17] Wenjun Jiang, Hongfei Xue, Chenglin Miao, Shiyang Wang, Sen Lin, Chong Tian, Srinivasan Murali, Haochen Hu, Zhi Sun, and Lu Su. Towards 3d human pose construction using wifi. In *International Conference on Mobile Computing and Networking (MobiCom)*, pages 1–14, 2020. 2, 3, 6, 7, 8
- [18] Diederik P. Kingma and Jimmy Ba. Adam: A method for stochastic optimization. In *International Conference on Learning Representations (ICLR)*, 2015. 6
- [19] Qiuqiang Kong, Yong Xu, Iwona Sobieraj, Wenwu Wang, and Mark D Plumbley. Sound event detection and time–frequency segmentation from weakly labelled data. *IEEE/ACM Transactions on Audio, Speech, and Language Processing*, 27(4):777–787, 2019. 4
- [20] Yuki Kubo, Yuto Koguchi, Buntarou Shizuki, Shin Takahashi, and Otmar Hilliges. AudioTouch: Minimally invasive sensing of micro-gestures via active bio-acoustic sensing. In *ACM International Conference on Mobile Human-Computer Interaction*, page 13, 2019. 3
- [21] Sohyun Lee, Jaesung Rim, Boseung Jeong, Geonu Kim, Byungju Woo, Haechan Lee, Sunghyun Cho, and Suha Kwak. Human pose estimation in extremely low-light conditions. In *IEEE/CVF Computer Vision and Pattern Recognition Conference (CVPR)*, pages 704–714, 2023. 1
- [22] Tianhong Li, Lijie Fan, Yuan Yuan, and Dina Katabi. Unsupervised learning for human sensing using radio signals. In *IEEE/CVF Winter Conference on Applications of Computer Vision (WACV)*, pages 3288–3297, 2022. 3
- [23] Wenhao Li, Hong Liu, Runwei Ding, Mengyuan Liu, Pichao Wang, and Wenming Yang. Exploiting temporal contexts with strided transformer for 3d human pose estimation. *IEEE Transactions on Multimedia*, 25:1282–1293, 2022. 1, 3

- [24] Ilya Loshchilov and Frank Hutter. Sgdr: Stochastic gradient descent with warm restarts. *arXiv preprint arXiv:1608.03983*, 2016. 7
- [25] Saif Mahmud, Ke Li, Guilin Hu, Hao Chen, Richard Jin, Ruidong Zhang, François Guimbretière, and Cheng Zhang. Posesonic: 3d upper body pose estimation through egocentric acoustic sensing on smartglasses. *ACM on Interactive, Mobile, Wearable and Ubiquitous Technologies (IMWUT)*, 7(3):1–28, 2023. 3
- [26] Mark D McDonnell and Wei Gao. Acoustic scene classification using deep residual networks with late fusion of separated high and low frequency paths. In *IEEE International Conference on Acoustics, Speech and Signal Processing (ICASSP)*, pages 141–145. IEEE, 2020. 4
- [27] Adiyana Mujibiyana, Xiang Cao, Desney S. Tan, Dan Morris, Shwetak N. Patel, and Jun Rekimoto. The sound of touch: On-body touch and gesture sensing based on transdermal ultrasound propagation. In *ACM Interactive Surfaces and Spaces Conference (ACM ISS)*, page 189–198, 2013. 3
- [28] Yusuke Oumi, Yuto Shibata, Go Irie, Akisato Kimura, Yoshimitsu Aoki, and Mariko Isogawa. Acoustic-based 3d human pose estimation robust to human position. *arXiv preprint arXiv:2411.07165*, 2024. 3
- [29] Manuel Palermo, Sara Moccia, Lucia Migliorelli, Emanuele Frontoni, and Cristina P. Santos. Real-time human pose estimation on a smart walker using convolutional neural networks. *Expert Systems With Applications*, 184(C), 2021. 1
- [30] Despoina Pavlidi, Symeon Delikaris-Manias, Ville Pulkki, and Athanasios Mouchtaris. 3d localization of multiple sound sources with intensity vector estimates in single source zones. In *European conference on signal processing (EU-SIPCO)*, pages 1556–1560. IEEE, 2015. 4
- [31] N Dinesh Reddy, Laurent Guigues, Leonid Pishchulin, Jayan Eledath, and Srinivasa G Narasimhan. Tesseract: End-to-end learnable multi-person articulated 3d pose tracking. In *IEEE/CVF Computer Vision and Pattern Recognition Conference (CVPR)*, pages 15190–15200, 2021. 1, 3
- [32] Yili Ren, Zi Wang, Yichao Wang, Sheng Tan, Yingying Chen, and Jie Yang. Gopose: 3d human pose estimation using wifi. *ACM on Interactive, Mobile, Wearable and Ubiquitous Technologies (IMWUT)*, 6(2), 2022. Publisher Copy-right: © 2022 ACM. 2, 3
- [33] Yuma Sakashita and Masaki Aono. Acoustic scene classification by ensemble of spectrograms based on adaptive temporal divisions. *Detection and Classification of Acoustic Scenes and Events (DCASE) Challenge*, 2018. 4
- [34] Yuto Shibata, Yutaka Kawashima, Mariko Isogawa, Go Irie, Akisato Kimura, and Yoshimitsu Aoki. Listening human behavior: 3d human pose estimation with acoustic signals. In *IEEE/CVF Computer Vision and Pattern Recognition Conference (CVPR)*, pages 13323–13332, 2023. 2, 3, 4, 6, 7, 8
- [35] Eli Shlizerman, Lucio Dery, Hayden Schoen, and Ira Kemelmacher-Shlizerman. Audio to body dynamics. In *IEEE/CVF Computer Vision and Pattern Recognition Conference (CVPR)*, pages 7574–7583, 2018. 3
- [36] Yang Song, Jascha Sohl-Dickstein, Diederik P Kingma, Abhishek Kumar, Stefano Ermon, and Ben Poole. Score-based generative modeling through stochastic differential equations. *arXiv preprint arXiv:2011.13456*, 2020. 3
- [37] Denis Tome, Patrick Peluse, Lourdes Agapito, and Hernan Badino. xr-egopose: Egocentric 3d human pose from an hmd camera. In *IEEE/CVF International Conference on Computer Vision (ICCV)*, pages 7728–7738, 2019. 1
- [38] Jonathan Tseng, Rodrigo Castellon, and Karen Liu. Edge: Editable dance generation from music. In *IEEE/CVF Computer Vision and Pattern Recognition Conference (CVPR)*, pages 448–458, 2023. 3
- [39] Mason Wang, Samuel Clarke, Jui-Hsien Wang, Ruohan Gao, and Jiajun Wu. Soundcam: a dataset for finding humans using room acoustics. *Conference on Neural Information Processing Systems (NeurIPS)*, 36, 2024. 3
- [40] Xudong Xu, Dejan Markovic, Jacob Sandakly, Todd Keebler, Steven Krenn, and Alexander Richard. Sounding bodies: Modeling 3d spatial sound of humans using body pose and audio. In *Conference on Neural Information Processing Systems (NeurIPS)*, pages 44740–44752, 2023. 3
- [41] Sicheng Yang, Zhiyong Wu, Minglei Li, Zhensong Zhang, Lei Hao, Weihong Bao, and Haolin Zhuang. Qpgesture: Quantization-based and phase-guided motion matching for natural speech-driven gesture generation. In *IEEE/CVF Computer Vision and Pattern Recognition Conference (CVPR)*, pages 2321–2330, 2023. 3
- [42] Zhijian Yang, Xiaoran Fan, Volkan Isler, and Hyun Soo Park. Posekernellifter: Metric lifting of 3d human pose using sound. In *IEEE/CVF Computer Vision and Pattern Recognition Conference (CVPR)*, pages 13179–13189, 2022. 2, 3
- [43] Masahiro Yasuda, Yuma Koizumi, Shoichiro Saito, Hisashi Uematsu, and Keisuke Imoto. Sound event localization based on sound intensity vector refined by dnn-based denoising and source separation. In *IEEE International Conference on Acoustics, Speech and Signal Processing (ICASSP)*, pages 651–655. IEEE, 2020. 4
- [44] Calvin Yeung, Kenjiro Ide, and Keisuke Fujii. Autosoccerpose: Automated 3d posture analysis of soccer shot movements. In *Proceedings of the IEEE/CVF Conference on Computer Vision and Pattern Recognition (CVPR) Workshops*, pages 3214–3224, 2024. 1
- [45] Hongwei Yi, Hualin Liang, Yifei Liu, Qiong Cao, Yandong Wen, Timo Bolkart, Dacheng Tao, and Michael J Black. Generating holistic 3d human motion from speech. In *IEEE/CVF Computer Vision and Pattern Recognition Conference (CVPR)*, pages 469–480, 2023. 3
- [46] Tomohiro Yokota and Tomoko Hashida. Hand gesture and on-body touch recognition by active acoustic sensing throughout the human body. In *Symposium on User Interface Software and Technology (UIST)*, page 113–115, 2016. 3
- [47] Mingmin Zhao, Tianhong Li, Mohammad Abu Alsheikh, Yonglong Tian, Hang Zhao, Antonio Torralba, and Dina Katabi. Through-wall human pose estimation using radio signals. In *IEEE/CVF Computer Vision and Pattern Recognition Conference (CVPR)*, pages 7356–7365, 2018. 2, 3
- [48] Ce Zheng, Wenhan Wu, Chen Chen, Taojiannan Yang, Si-jie Zhu, Ju Shen, Nasser Kehtarnavaz, and Mubarak Shah.

Deep learning-based human pose estimation: A survey. *ACM Computing Surveys*, 56(1):1–37, 2023. 1, 3

- [49] Lingting Zhu, Xian Liu, Xuanyu Liu, Rui Qian, Ziwei Liu, and Lequan Yu. Taming diffusion models for audio-driven co-speech gesture generation. In *IEEE/CVF Computer Vision and Pattern Recognition Conference (CVPR)*, pages 10544–10553, 2023. 3